



Core-shell particles as efficient broadband absorbers in infrared optical range

ANDREY B. EVLYUKHIN,^{1,*} KHACHATUR V. NERKARARYAN,² AND SERGEY I. BOZHEVOLNYI³

¹*Institute of Quantum Optics, Leibniz Universität Hannover, 30167 Hannover, Germany*

²*Department of Physics, Yerevan State University, 375049 Yerevan, Armenia*

³*Centre for Nano Optics, University of Southern Denmark, Campusvej 55, DK-5230 Odense M, Denmark*

**a.b.evlyukhin@daad-alumni.de*

Abstract: We demonstrate that efficient broadband absorption of infrared radiation can be obtained with deeply subwavelength spherical dielectric particles covered by a thin metal layer. Considerations based on Mie theory and the quasi-static approximation reveal a wide range of configuration parameters, within which the absorption cross section reaches the geometrical one and exceeds more than by order of magnitude the scattering cross section in the infrared spectrum. We show that the absorption is not only efficient but also broadband with the spectral width being close to the resonant wavelength corresponding to the maximum of the absorption cross section. We obtain a simple analytical expression for the absorption resonance that allows one to quickly identify the configuration parameters ensuring strong infrared absorption in a given spectral range. Relation between the absorption resonance and excitation of the short-range surface plasmon modes in the metal shell of particles is demonstrated and discussed. Our results can be used as practical guidelines for realization of efficient broadband infrared absorbers of subwavelength sizes desirable in diverse applications.

© 2019 Optical Society of America under the terms of the [OSA Open Access Publishing Agreement](#)

1. Introduction

Electromagnetic radiation absorbers are components in which the incident radiation at operating wavelengths can be efficiently absorbed and then transformed into ohmic heat or other forms of energy. Thereby, neither transmission nor reflection is produced when a wave passes through a perfect absorber. Recent advances in plasmonics and metamaterials research together with the progress in nanotechnology, especially in nanofabrication techniques, resulted in the development of novel configurations of electromagnetic absorbers. These absorbers utilize localized surface plasmon polaritons and often involve metamaterial-based approaches to achieve smaller absorber volumes, sufficiently efficient performance along with the design flexibility based on configuration geometry rather than materials used [1–7]. Practically perfect absorbers have been realized within a wide range of frequencies, including terahertz [8], microwave [9], infrared [10] and optical [11] band have been investigated. Absorbers targeting specific characteristics, such as, for example, polarization insensitive [12], wide-angle [13], multi-band [14] and broadband absorption [15], have been developed by exploiting different design approaches. Moreover, multi-band [16] or broadband [17] absorbers that are simultaneously insensitive to the polarization and feature wide-angle have also been demonstrated experimentally. One would however like to simplify the absorber design while keeping these attractive features, although the requirement of polarization and angle insensitive performance severely narrows the range of possible configurations.

Design challenges increase significantly when considering the infrared absorbers, because plasmonic characteristics of metal-based configurations deteriorate rapidly for long wavelengths [18]. Thus, it is well-known that at low frequencies, due to sharp increases in metal dielectric constants and especially in their imaginary parts, unique properties of localized surface plasmons practically disappear, resulting (among other things) in a drastic decrease of the radiation

absorption by individual small metal particles [19]. This behaviour significantly restricts the usage of small metal particles as effective radiation absorbers in the infrared range. In general, small particles would efficiently absorb radiation only when their dielectric constants are of the same order as those of their environment, otherwise incident electromagnetic fields do not penetrate the material of particles [20]. Realizing that this material matching can be facilitated by using composite materials, one is led to the idea of exploiting core-shell (dielectric-metal) particles for efficient and isotropic infrared absorption. Note that the localized surface plasmon resonance of core-shell spherical structures has been a subject of numerous investigations during last two decades, notably for exploring its tunability [21, 22] and implementation of "cloaking" effects [23, 24].

In this article we show that the resonant efficient and broadband absorption of electromagnetic radiation can be obtained in the infrared spectral range by tuning the geometrical and material parameters of spherical metal-coated dielectric particles. In the search for efficient isotropic infrared absorbers, we identify a special range of parameters of core-shell dielectric-metal spherical particles of subwavelength sizes [21, 22], viz., nm-thin shells of "bad" metals with approximately equal in magnitude real and imaginary parts of dielectric constants, that allows one to realize subwavelength-sized isotropic, efficient and broadband infrared absorbers with negligibly small scattering properties (the latter can also be important for some applications). We also derive a simple and yet accurate (in the aforementioned parameter range) relationship that allows one to quickly identify the configuration parameters needed for the practical realization of the efficient absorption in a given wavelength range and with given materials. Moreover, we demonstrate that the absorption resonance of nm-thin-shell (core-shell) subwavelength-sized particles is connected with the excitation of short-range surface plasmon modes [25] excited in the particle shells, which is a novel and important physical interpretation of light interaction with nm-thin-shell metal-dielectric particles. Note that, in general, short-range plasmon (slow-plasmon) investigations attract significant research attention at present time [26].

We use two well established theoretical methods (Mie theory and the quasi-static approximation) in our investigations of the absorption properties of the core-shell particles in the infrared. This approach allowed us to cross check the accuracy of the quasi-static approximation, which is important for arriving at the simple design relationship that we established in our article.

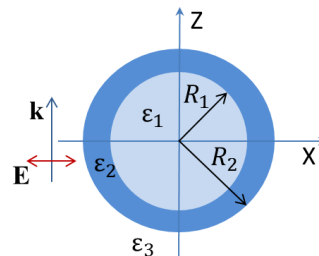


Fig. 1. Nanoshell particle parameters: ϵ_1 , ϵ_2 , and ϵ_3 are the dielectric permittivities of the core, shell, and environment medium, respectively, R_1 is the core radius, and R_2 is the total particle radius. \mathbf{k} and \mathbf{E} are the wavevector and electric field of an incident plane wave.

2. Theoretical model

Let's consider plane wave scattering by a spherical shell particle with parameters shown in Fig. 1. In the quasi-static approximation ($kR_2 \ll 1$, where k is the wavenumber in environment medium with ϵ_3) the dipole moment of particle is determined by the following expression [21]

$$\mathbf{p} = 4\pi\epsilon_0\epsilon_3R_2^3\chi\mathbf{E}, \quad (1)$$

where \mathbf{E} is the incident wave electric field at the particle centre, ε_0 is the vacuum dielectric constant,

$$\chi = \frac{(1 + 2\eta y)\varepsilon_2 - (1 - \eta y)\varepsilon_3}{(1 + 2\eta y)\varepsilon_2 + 2(1 - \eta y)\varepsilon_3}. \quad (2)$$

Here

$$y = \frac{\varepsilon_1 - \varepsilon_2}{\varepsilon_1 + 2\varepsilon_2}, \quad \eta = \frac{R_1^3}{R_2^3}.$$

The electric dipole polarizability α of the particle is determined by the expression $\mathbf{p} = \alpha\mathbf{E}$. The extinction cross section σ_{ext} in the dipole approximation is

$$\sigma_{ext} = \frac{k_0}{\varepsilon_0\sqrt{\varepsilon_3}}\text{Im}\alpha, \quad (3)$$

where k_0 is the wavenumber in vacuum. Inserting in Eq. (3) the polarizability in quasi-static approximation one obtains the absorption cross section

$$\sigma_{abs} = 4\pi k_0\sqrt{\varepsilon_3}R_2^3\text{Im}\chi. \quad (4)$$

For the scattering cross section we obtain

$$\sigma_{sca} = \frac{k_0^4}{3}8\pi\varepsilon_3^2R_2^6|\chi|^2. \quad (5)$$

Assuming that

$$|\varepsilon_2| \gg \varepsilon_1, \varepsilon_3 \quad (6)$$

and using that $y = -1/2 + 3\varepsilon_1/(4\varepsilon_2)$ we get

$$\text{Im}\chi \approx \frac{18(1 - \eta)\varepsilon_3\varepsilon_2''}{[3(\varepsilon_1 + 2\varepsilon_3) + 2(1 - \eta)\varepsilon_2']^2 + 4(1 - \eta)^2\varepsilon_2''^2} \quad (7)$$

and

$$|\chi|^2 \approx \frac{[3(\varepsilon_1 - \varepsilon_3) + 2(1 - \eta)\varepsilon_2']^2 + 4(1 - \eta)^2\varepsilon_2''^2}{[3(\varepsilon_1 + 2\varepsilon_3) + 2(1 - \eta)\varepsilon_2']^2 + 4(1 - \eta)^2\varepsilon_2''^2} \quad (8)$$

where $\varepsilon_2 = \varepsilon_2' + i\varepsilon_2''$. The absorption resonant condition is

$$2(1 - \eta)|\varepsilon_2'| = 3(\varepsilon_1 + 2\varepsilon_3) \rightarrow (1 - \eta) = \frac{3(\varepsilon_1 + 2\varepsilon_3)}{2|\varepsilon_2'|}, \quad (9)$$

where we assumed that $(-\varepsilon_2') > 0$. For $\eta \sim 1$ the resonant condition Eq. (9) can be rewritten as

$$\Delta_S = R_2 \frac{\varepsilon_1 + 2\varepsilon_3}{2|\varepsilon_2'|}, \quad (10)$$

where Δ_S is the thickness of the particle's shell. At the resonance condition, the absorption and scattering cross sections become as follows

$$\sigma_{abs}^R = 4\pi k_0\sqrt{\varepsilon_3}R_2^3 \frac{3\varepsilon_3|\varepsilon_2'|}{(\varepsilon_1 + 2\varepsilon_3)\varepsilon_2''}, \quad (11)$$

$$\sigma_{sca}^R = \frac{8}{3}\pi k_0^4\varepsilon_3^2R_2^6 \left(1 + \frac{9\varepsilon_3^2\varepsilon_2''^2}{(\varepsilon_1 + 2\varepsilon_3)^2\varepsilon_2''^2} \right), \quad (12)$$

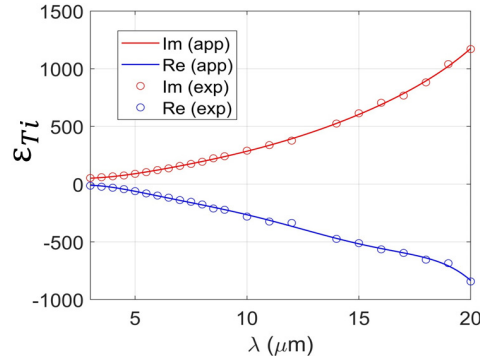


Fig. 2. Dielectric permittivity of Ti. "exp" means the experimental values from [27]; "app" means the polynomial approximation.

respectively. Estimating the ratio $\sigma_{abs}^R/\sigma_{sca}^R$ one arrives at the additional condition that should be imposed on the shell material for the absorption to significantly exceed the scattering. Considering $|\varepsilon_2'| \approx \varepsilon_2''$ one obtains $\sigma_{abs}^R/\sigma_{sca}^R \sim 1/(k_0 R_2)^3 \gg 1$, i.e., the absorption dominates the scattering for relatively small particles. For good metals with $|\varepsilon_2'| \gg \varepsilon_2''$, one obtains $\sigma_{abs}^R/\sigma_{sca}^R \sim [1/(k_0 R_2)^3][\varepsilon_2''/|\varepsilon_2'|]$, so that the absorption and scattering cross sections can have similar values, if $[1/(k_0 R_2)^3][\varepsilon_2''/|\varepsilon_2'|] \sim 1$. Thus, for the realization of strong and dominant absorption, one should choose poor shell metals with $|\varepsilon_2'|/\varepsilon_2'' \sim 1$. Additionally, as follows from the resonant condition Eq. (10), the resonant shell thickness $\Delta_S \sim R_2/|\varepsilon_2'|$ and may formally become very (nonphysically) thin for materials with extremely large $|\varepsilon_2'|$. Here we assumed that ε_1 and ε_3 correspond to dielectrics and do not significantly differ from that of air or glass.

The above analysis demonstrates that the resonant light absorption could be implemented in different spectral ranges where the quasi-static approach is applicable and the condition Eq. (10) is satisfied. Note, that at deep subwavelength dimensions, nanoresonators can often be viewed as "Fabry-Perot cavities" involving slow-plasmon modes that, at resonance, form standing waves being reflected at structure terminations [25, 26]. It might however be difficult to directly link these two interpretations for curved geometries because of lack of corresponding expressions for slow-plasmon modes. The quasi-static expression for the slow-plasmon mode (short-range surface plasmon polariton) propagation constant real part in a *planar* dielectric-metal-dielectric configuration reads [28]:

$$\beta \simeq \frac{\varepsilon_1 + \varepsilon_3}{\Delta_S |\varepsilon_2'|}. \quad (13)$$

Requiring that $\beta \pi R = 2\pi$ with R being the average of the two radii ($R = [R_1 + R_2]/2$) leads to the resonance condition in the form:

$$\Delta_S \simeq R \frac{\varepsilon_1 + \varepsilon_3}{2|\varepsilon_2'|}. \quad (14)$$

We think that the difference of this expression and the condition Eq. (10) can be attributed to the difference in the slow-plasmon mode propagation constants for planar and spherical geometries. At the same time, the scaling with respect to the most important configuration parameters, the shell thickness, particle radius and metal constant, is identical: the resonance position is preserved if $\Delta_S |\varepsilon_2'| R^{-1} \simeq \text{const}$.

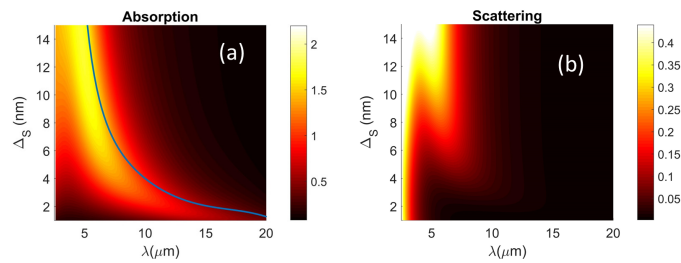


Fig. 3. (a) Spectra of the absorption efficiency calculated by Mie theory for particles with $R_1 = 500$ nm and different Ti -shell thickness Δ_S . (b) Corresponding spectra of the scattering efficiency. The blue line in (a) corresponds to the absorption resonance calculated in the quasi-static approximation. Note that the scale of (b) is decreased by 5 times compared to that of (a).

3. Results

The relatively simple condition Eq. (10) derived above allows one to quickly identify the configuration parameters ensuring strong infrared absorption in a given spectral range. In order to get the strong absorption in the infra-red region we consider a dielectric particle with $R_1 = 500$ nm, $\epsilon_1 = 2.25$, and covered by a thin titanium (Ti) shell. The Ti dielectric permittivity $\epsilon_2 = \epsilon_{Ti}$ is presented in Fig. 2. For example, $\epsilon_{Ti} = -281 + i290$ for the wavelength $\lambda = 10 \mu\text{m}$. Applicability of the quasi-static approximation is checked by comparisons of results with calculations in the frame of Mie theory [20]. It should be mentioned that, as far as the choice of dielectric core materials is concerned, there exist various materials, for example KBr , KCl , BaF_2 , $NaCl$ and others, for which $\epsilon_1 \approx 2.25$ in the broad spectral range around $\lambda \sim 10 \mu\text{m}$ [29].

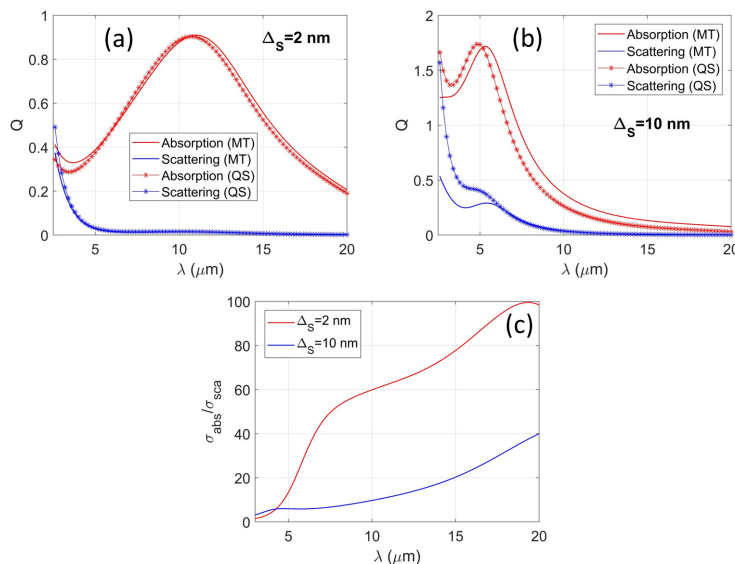


Fig. 4. (a) and (b) The scattering and absorption efficiencies for the Ti -shell-core spherical particles calculated by Mie theory (MT) and the quasi-static approximations (QS). Δ_S is the thickness of the Ti -shell. The parameters of the system are presented in the main text. (c) Ratios between the absorption and scattering cross sections. The particles are located in air with $\epsilon_3 = 1$.

Figure 3 demonstrates the absorption and scattering efficiencies Q (the absorption and scattering cross sections divided by the area of particle geometrical section πR_2^2) calculated using Mie theory for different wavelengths λ of incident waves and for different shell thickness Δ_S . One can see that the absorption significantly exceeds the scattering in the considered spectral range with the absorption becoming progressively dominant for longer wavelengths. Positions of the absorption resonance obtained from Eq. (10) and presented in Fig. 3(a) by a blue line agree with the general calculations.

From the results presented in Fig. 4 one can see that description of the absorption resonance in the quasi-static approximation provides best agreement with Mie theory for particle with very thin shells Fig. 4(a). In this case the resonant absorption is realized in a broad ($\Delta\lambda = 10\mu\text{m}$) spectral region around $\lambda = 10\mu\text{m}$ and its maximum efficiency is equal to almost 1. With increasing of Δ_S the resonance is shifted to the blue side with decreasing of its width (Fig. 4(b)). However, the relation between the resonant wavelength λ_R and the width of absorption band $\Delta\lambda \approx \lambda_R$ is preserved. Spectral development of the ratio between absorption and scattering cross sections is presented in Fig. 4(c). When the shell thickness is 2 nm, the resonance absorption cross section is 60 times larger than the scattering cross section. This difference strongly decreases with increase of the particle shell: for $\Delta_S = 10$ nm this ratio is equal to only 5. Interestingly to note that the resonant absorption and scattering efficiencies grow very fast when increasing the particle shell thickness. Moreover, the scattering cross section increases faster than the absorption cross section. Such behaviour demonstrates that the strong absorption effect for thin shell particles can be considered as a configuration resonance of the total structure. The relative absorption increase for thinner shells can be attributed to the increase of damping of slow-plasmon modes.

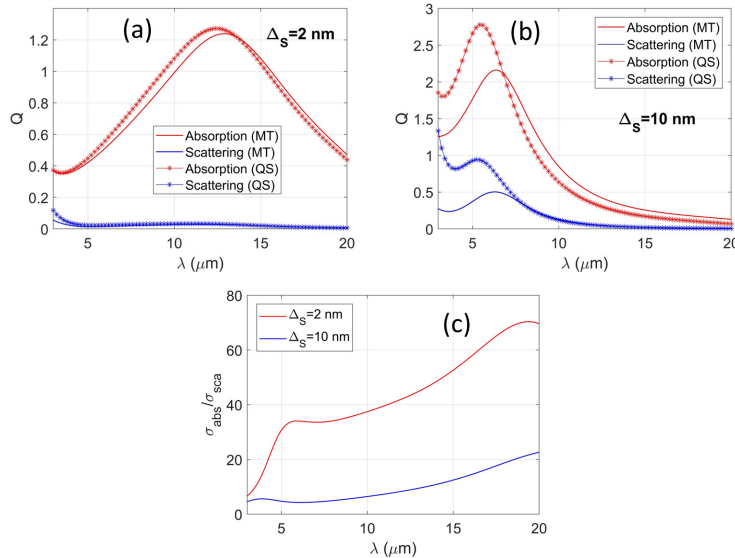


Fig. 5. (a) and (b) The scattering and absorption efficiencies for the Ti -shell-core spherical particles calculated by Mie theory (MT) and the quasi-static approximations (QS). Δ_S is the thickness of the Ti -shell. (c) Ratios between the absorption and scattering cross sections. The parameters of the system are presented in the main text. The particles are located in medium with $\epsilon_3 = 1.69$. The wavelengths are shown in vacuum.

Importantly that the considered effect is also observed for the cases when particles are located in dielectric medium with $\epsilon_3 \neq 1$. Results presented in Fig. 5 confirm this. With increasing of ϵ_3 the absorption efficiency Q increases too and can exceed the efficiency for air environment.

Here we can again observe large differences between the resonant absorption and scattering cross sections (Fig. 5(c)) for small shell thicknesses as a consequence of the configuration resonance.

Concluding, let us consider what absorption and scattering properties in the infrared can be obtained for the shells made of gold, *Au*, a metal which is frequently in plasmonics. Figure 6 presents the absorption and scattering efficiencies calculated with Mie theory for dielectric particles ($\epsilon_1 = 2.25$) covered by *Au*-shells ($\epsilon_2 = \epsilon_{Au}$). Dielectric permittivity of gold in the infrared is taken from [30]. In contrast to the *Ti*-shells, the *Au*-shells do not ensure the dominance of resonant absorption over scattering (compare Fig 6(a) and Fig. 6(b)) for the reasons discussed above in the section "Theoretical model". Gold exhibits too large differences between $|\epsilon'_2|$ and ϵ''_2 in the considered spectral range (for example, $\epsilon_2 \approx -755 + i107$ for $\lambda \approx 4 \mu\text{m}$). Moreover, for large wavelengths (larger than $\lambda \approx 5 \mu\text{m}$ in Fig. 6(a)) the resonant shell thicknesses become smaller than 1 nm because of rapid increase of $|\epsilon'_2|$ for gold (for example, $|\epsilon'_2| \approx 2244$ for $\lambda \approx 7 \mu\text{m}$, and $|\epsilon'_2| \approx 4326$ for $\lambda \approx 10 \mu\text{m}$.) One can therefore conclude that the usage of *Au* is very problematic for realization of broadband absorbers in the infrared optical range.

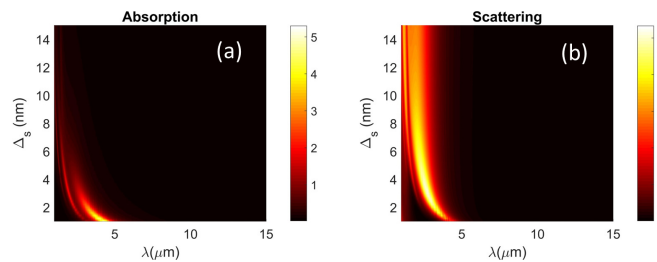


Fig. 6. (a) and (b) Spectra of the absorption and scattering efficiency calculated by Mie theory for particles with $R_1 = 350 \text{ nm}$ and different *Au*-shell thickness Δ_S . The particles with $\epsilon_1 = 2.25$ are located in medium with $\epsilon_3 = 1$.

4. Conclusion

In summary, it has been shown, that subwavelength spherical dielectric particles covered with a thin metal layer can serve as a very effective absorber in the infrared spectral range. An important feature of such absorbers with spherical symmetry is their independence on the angular and polarization orientation of the incident radiation. In addition, a simple analytical model and expressions, obtained in the quasi-static approximation for description of the absorption resonance, can be used for identification of the configuration parameters required for the implementation of strong absorption in a given spectral range. It has further been shown that the demonstrated absorption resonance can be realized for medium having different dielectric constants, an important feature that expands application perspectives of the investigated structures. Moreover, it has also been revealed that the absorption resonance is connected with the excitation of short-range surface plasmon modes excited in the particle shells. We believe that our results provide new important information and practical guidelines for the realization of subwavelength-sized isotropic, efficient and broadband infrared absorbers with negligibly small scattering properties utilizing the excitation of short-range plasmon modes.

Funding

European Research Council (341054) (PLAQNAP); University of Southern Denmark (SDU 2020), Deutsche Forschungsgemeinschaft (DFG, German Research Foundation) under Germany's Excellence Strategy within the Cluster of Excellence PhoenixD (EXC 2122, Project ID 390833453).

References

1. N. I. Landy, S. Sajuyigbe, J. J. Mock, D. R. Smith, and W. J. Padilla. "Perfect Metamaterial Absorber," *Phys. Rev. Lett.* **100**, 207402 (2008).
2. K Aydin, V. E. Ferry, R. M. Briggs, and H. A. Atwater, "Broadband polarization-independent resonant light absorption using ultrathin plasmonic super absorbers," *Nat Commun.*, **2**, 517 (2011).
3. X. L. Liu, T. Starr, A. F. Starr, and W. J. Padilla, "Infrared spatial and frequency selective metamaterial with near-unity absorbance," *Phys. Rev. Lett.* **104**, 207403 (2010).
4. T. Søndergaard, S. M. Novikov, T. Holmgaard, R. L. Eriksen, J. Beermann, Z. Han, K. Pedersen, and S. I. Bozhevolnyi, "Plasmonic black gold by adiabatic nanofocusing and absorption of light in ultra-sharp convex grooves," *Nat. Commun.* **3**, 969 (2012).
5. C. M. Watts, X. Liu, and W. J. Padilla, "Metamaterial electromagnetic wave absorbers," *Adv. Mater.* **24**, OP98-OP120 (2012).
6. Y. Cui, Y. He, Y. Jin, F. Ding, L. Yang, Y. Ye, S. Zhong, Y. Lin, and S. He, "Plasmonic and metamaterial structures as electromagnetic absorbers," *Laser Photonics Rev.* **8**, 495–520 (2014).
7. S. Ogawa and M. Kimata. "Metal-insulator-metal-based plasmonic metamaterial absorbers at visible and infrared Wavelengths: A Review," *Materials* **11**, 458 (2018).
8. Q. Y. Wen, H. W. Zhang, Y. S. Xie, Q. H. Yang, and Y. L. Liu, "Dual bandterahertz metamaterial absorber: Design, fabrication, and characterization," *Appl. Phys. Lett.* **95**, 241111 (2009).
9. F. Ding, Y. X. Cui, X. C. Ge, Y. Jin, and S. L. He, "Ultra-broadband microwave metamaterial absorber," *Appl. Phys. Lett.* **100**, 103506 (2012).
10. N. Liu, M. Mesch, T. Weiss, M. Hentschel, and H. Giessen, "Infrared perfect absorber and its application as plasmonic sensor," *Nano Lett.* **10**, 2342–2348 (2010).
11. C. H. Lin, R. L. Chern, and H. Y. Lin, "Polarization-independent broadband nearly perfect absorbers in the visible regime," *Opt Express* **19**, 415–424 (2011).
12. Y. Q. Ye, Y. Jin, and S. L. He, "Omnidirectional, polarization-insensitive and broadband thin absorber in the terahertz regime," *J. Opt. Soc. Am. B.* **3**, 498–504 (2010).
13. C. W. Cheng, M. N. Abbas, C. W. Chiu, K. T. Lai, M. H. Shih, and Y. C. Chang, "Wide-angle polarization independent infrared broadband absorbers based on metallic multisized disk arrays," *Opt. Express* **20**, 10376–10381 (2012).
14. B. Y. Zhang, J. Hendrickson, and J. P. Guo, "Multispectral near-perfect metamaterial absorbers using spatially multiplexed plasmon resonance metal square structures," *J. Opt. Soc. Am. B.* **30**, 656–662 (2013).
15. P. Bouchon, C. Koechlin, F. Pardo, R. Haïdar, and J. L. Pelouard, "Wideband omnidirectional infrared absorber with a patchwork of plasmonic nanoantennas," *Opt Lett.* **37**, 1038–1040 (2012).
16. X. Shen, T. J. Cui, J. Zhao, H. F. Ma, W. X. Jiang, and H. Li, "Polarization-independent wide-angle triple-band metamaterial absorber," *Opt. Express*, **19**, 9401–9407 (2011).
17. S. Q. Chen, H. Cheng, H. F. Yang, J. J. Li, X. Y. Duan, C. Z. Gu, and J. G. Tian, "Polarization insensitive and omnidirectional broadband near perfect planar metamaterial absorber in the near infrared regime," *Appl. Phys. Lett.* **99**, 253104 (2011).
18. T. Maurer, P.-M. Adam, and G. Lévêque, "Coupling between plasmonic films and nanostructures: from basics to applications," *Nanophoton.* **4**, 363–382 (2015).
19. L. D. Landau and E. M. Lifshitz, *Electrodynamics of Continuous Media*, (Pergamon Press, 1960), (Volume 8 of A Course of Theoretical Physics).
20. C. F. Bohren and D. R. Huffman, *Absorption and Scattering of Light by Small Particles* (Wiley, New York, 1983).
21. R. D. Averitt, S. L. Westcott, and N. J. Halas, "Linear optical properties of gold nanoshells," *J. Opt. Soc. Am. B* **16**, 1824–1832 (1999).
22. N. J. Halas, S. Lal, Wei-Shun Chang, S. Link, and P. Nordlander, "Plasmons in strongly coupled metallic nanostructures," *Chem. Rev.* **111**, 3913–3961 (2011).
23. A. Alú and N. Engheta, "Achieving transparency with plasmonic and metamaterial coatings," *Phys. Rev. E* **72**, 016623 (2005).
24. A. Alú and N. Engheta, "Plasmonic materials in transparency and cloaking problems: mechanism, robustness, and physical insights," *Opt. Express* **15**, 3318–3332 (2007).
25. T. Søndergaard and S. Bozhevolnyi, "Slow-plasmon resonant nanostructures: Scattering and field enhancements," *Phys. Rev. B* **75**, 073402 (2007).
26. P. Lalanne, S. Coudert, G. Duchateau, S. Dilhaire, and K. Vynck, "Structural slow waves: parallels between photonic crystals and plasmonic waveguides," *ACS Photonics* **6**, 4–17 (2019).
27. M. A. Ordal, L. L. Long, R. J. Bell, S. E. Bell, R. R. Bell, R. W. Alexander, Jr., and C. A. Ward, "Optical properties of the metals Al, Co, Cu, Au, Fe, Pb, Ni, Pd, Pt, Ag, Ti, and W in the infrared and far infrared," *Appl. Opt.* **22**, 1099–1120 (1983).
28. E. N. Economou, "Surface plasmons in thin films," *Phys. Rev.* **182**, 539–554 (1969).
29. www.photonics.com/Articles/Optical_Materials_Transmission_and_Refractive/a25498
30. R. L. Olmon, B. Slovick, T. W. Johnson, D. Shelton, S.-H. Oh, G.D. Boreman, and M. B. Raschke, "Optical dielectric function of gold," *Phys. Rev. B* **86**, 235147 (2012).